Ordered Structure of Poly(1*H*,1*H*-fluoroalkyl α-fluoroacrylate)s

Tetsuo Shimizu,* Yoshito Tanaka, Shoichi Kutsumizu,† and Shinichi Yano†

R & D Department, Daikin Industries Ltd., Settsu, Osaka 566, Japan

Received May 31, 1995; Revised Manuscript Received September 19, 1995[⊗]

ABSTRACT: Structural studies for a homologous series of poly(1*H*,1*H*-fluoroalkyl α-fluoroacrylate)s [−{$CH_2CFC(O)OCH_2(CF_2)_nY$}$_p$−, Y = H or F, Nc = 1 + *n* = 2−12] have been performed with X-ray diffraction, differential scanning calorimetric, and polarized IR spectral measurements. At room temperature, all the homologues used have an ordered structure (crystallites) which consists of the ordering of main and fluoroalkyl side chains. The structure of crystallites depended on both length (N_c) of fluoroalkyl side chains and chemical structure. In the shorter fluoroalkyl homologues (N_c < 7), the side chains are arranged in a double-layer packing at room temperature, while they are mostly in a single-layer packing in the longer fluoroalkyl homologues. As temperature increased, in the short fluoroalkyl homologues, the double-layer packing was more arranged around a temperature above T_g and then gradually disturbed, while in the long fluoroalkyl homologues, the single layer packing transformed into a double-layer packing above T_g. The layered structure and its change with temperature were discussed from the degree of orderings of the main backbone chains and the fluoroalkyl side chains.

Introduction

Fluoroalkyl acrylate, methacrylate, and α-haloacrylate polymers are comb-shaped polymers functionalized with fluoroalkyl ester chains, and have recently received scientific interest because of their characteristic structure and properties. Structural studies for poly(fluoroalkyl acrylate)s (PA-Hm-Fn-Y, Y = H or F) and poly(fluoroalkyl methacrylate)s (PM-Hm-Fn-Y, Y = H or F) have been done by several researchers.[1−6] The notation for polymers described in this paper is shown in Figure 1, where the number of CH_2 moieties (*m*) is usually 1 or 2. When the number of CF_2 moieties (*n*) in *n*-fluoroalkyl side chains is larger than or equal to 7, or the carbon number (N_c) of the side chains is not less than 8, the fluoroalkyl side chains tend to crystallize in the polymer matrix to form a layered structure. Moreover the layered structure depended on not only the length of fluoroalkyl chains but also temperature. According to the recent work of Volkov et al.,[5] PA-H2-F8-F forms a double-layer packing of fluoroalkyl side chains at room temperature, while PM-H2-F8-F has both double- and single-layered structures. The double- and single-layer packings in PM-H2-F8-F transformed into a single-layer packing between 366 and 388 K with increasing temperature.

In the previous communication for poly(fluoroalkyl α-fluoroacrylate)s (PF-H1-Fn-Y, Y = H or F),[7] we reported that the crystallites are formed even in the short fluoroalkyl homologues such as PF-H1-F1-F and PF-H1-F2-F in which N_c (=1 + *n*) is 2 and 3, respectively, much smaller than 8, and that not only the fluoroalkyl side chains but the main backbone chains also participate in the crystallization. We also studied the ordered structure for four PX-H2-F8-F whose X are H, CH_3, F, and Cl to clarify how the substituent (X) at the α-position of acrylate moiety affects the structure of crystallites.[8] All the polymers had crystallites formed by the 1*H*,1*H*,2*H*,2*H*-perfluorodecyl side chains at room temperature; PA-H2-F8-F and PM-H2-F8-F formed the double-layer packing of the side chains and both double- and single-layer packings, respectively, while PF-H2-F8-F and PC-H2-F8-F prefered to form a single-layer packing. As temperature increased, the single-layer packings of PF-H2-F8-F and PC-H2-F8-F transformed into the double-layer packings, followed by melting of the side-chain crystallites. These past results suggest that the formation of crystallites and their structure are governed by the chemical structure and length of fluoroalkyl side chains and the α-substituent of the acrylate moiety.

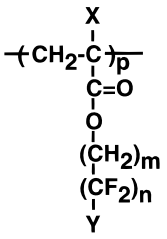

Figure 1. Chemical structure of polymers denoted PX-Hm-Fn-Y, where X = H, CH_3, F, or Cl and Y = H or F. The carbon number (N_c) of fluoroalkyl side chains is *m* + *n*.

In general, PX-Hm-Fn-Y polymers are known to be transparent and to have low refractive index, low surface free energy, and high solubility, some of which may be certainly functionalized with the fluoroalkyl groups. To date, taking advantage of these useful physical properties, these polymers have been industrially used as oil and water repellent agents, moisture-proof coatings, and clad materials for polymeric optical fibers. Of course, these functional properties should be influenced by the existence of crystallites.

The interesting results mentioned above strongly draw our attention to clarify how and why PX-Hm-Fn-Y polymers have important and sometimes unique ordered structures and properties. In this paper, we report systematical and detailed studies on ordered structures for a homologous series of poly(1*H*,1*H*-fluoroalkyl α-fluoroacrylate)s (PF-H1-Fn-Y, Y = H or F). The formation and structure of crystallites and their transformation with temperature are discussed on the basis of length and chemical structure of the fluoroalkyl side chains and the substituent (X) at the α-position of acrylate moiety. It is found that the formation and structure of crystal-

* To whom correspondence should be addressed.
† Department of Chemistry, Faculty of Engineering, Gifu University, Yanagido, Gifu 501-11, Japan.
⊗ Abstract published in *Advance ACS Abstracts,* November 15, 1995.

0024-9297/96/2229-0156$12.00/0

Table 1. Characteristic Values for the Polymers Synthesized

	triad tacticity[a] (±0.02)				
polymer	mm	mr	rr	M_w,[b] × 10^5	[η],[c] dL g^{-1}
PF-H1-F1-F	0.13	0.50	0.37	2.6	0.678
PF-H1-F2-H	0.12	0.47	0.41	2.2	0.525
PF-H1-F2-F	0.12	0.48	0.40	1.8	0.533
PF-H1-F3-F	0.11	0.49	0.40	ND[d]	0.185
PF-H1-F4-H	0.11	0.48	0.41	7.0	0.990
PF-H1-F4-F	0.12	0.46	0.42	ND	ND
PF-H1-F6-H	0.13	0.46	0.41	4.4	0.569
PF-H1-F7-F	0.12	0.48	0.40	ND	ND
PF-H1-F8-H	0.11	0.56	0.33	3.7	0.272
PF-H1-F8-F	0.13	0.46	0.41	ND	ND
PF-H1-F9-F	0.12	0.45	0.43	ND	ND
PF-H1-F11-F	0.11	0.47	0.42	ND	ND
PM-H1-F1-F	0.07	0.41	0.52	3.5	0.747
PM-H1-F2-H	0.07	0.38	0.55	7.3	0.909
PM-H1-F2-F	0.06	0.40	0.54	2.8	0.437
PM-H1-F4-H	0.06	0.42	0.52	7.7	0.801
PM-H1-F8-F	0.06	0.40	0.54	ND	ND
PA-H1-F1-F	0.02	0.61	0.37	4.8	0.107
PA-H1-F2-F	0.03	0.60	0.37	2.3	0.103

[a] mm, isotactic; mr, heterotactic; rr, syndiotactic. [b] Weight-average molecular weights measured by GPC using THF. [c] Intrinsic viscosity at 308 K using ethyl acetate. [d] Not determined, because of insolubility in the solvents.

lites are closely connected with the ordering of two segments, the fluoroalkyl side chain and the acrylate backbone chain.

Experimental Section

1*H*,1*H*-Fluoroalkyl α-fluoroacrylate monomers were prepared by a dehydrogen fluoride reaction of α-fluoroacryloyl fluoride with the corresponding fluoroalcohols [$HOCH_2(CF_2)_nF$/H]. 1*H*,1*H*-Fluoroalkyl methacrylates and the acrylates were prepared by a dehydrogen chloride reaction of the methacryloyl and acryloyl chlorides with the corresponding alcohols. All monomers synthesized above were distilled and confirmed to have a purity of 98% or higher by gas chromatography. The PX-H1-Fn-Y polymers were obtained by a radical polymerization at 323 K for PF-H1-Fn-Y and at 343 K for PA-H1-Fn-Y and PM-H1-Fn-Y, using 2,2′-azobis(isobutyronitrile) (AIBN) as an initiator and isooctyl mercaptoacetate or lauryl mercaptan as a molecular weight regulator in a Pyrex tube in which a 1,3-bis(trifluoromethyl)benzene solution of the corresponding monomer and other ingredients were sealed after deairing under liquid nitrogen. The polymers obtained were heated at 453−533 K under a reduced pressure for 24 h to remove unreacted monomers and other volatiles and used without further purification. Elemental analyses were carried out by an element analyzer (Yanaco CHN CORDER MT-5) and a fluoride-selective electrode (ORION RESEARCH microprocessor ionalyzer 901) to confirm the purity. The polymers were compression-molded into sheets about 0.5 mm thick at a temperature above melting point (T_m). The sheets obtained were cooled to room temperature at a rate of about 0.3 K min^{-1} after heating enough above T_m. The oriented samples were prepared by uniaxially drawing to a ratio of ∼4 at a temperature above glass transition (T_g). Characteristic values of the polymers synthesized here are listed in Table 1. Weight-average molecular weights (M_w) were determined by gel permeation chromatography using tetrahydrofuran (THF) as an eluent and polystyrene as a standard, and intrinsic viscosities [η] (dL g^{-1}) were measured in ethyl acetate at 308 K by use of an Ubbelohde viscometer. The values of M_w range from 1.8 × 10^5 to 7.7 × 10^5 and [η] values are between 0.10 and 0.99 dL g^{-1}, indicating that the polymer samples had high enough molecular weight to be regarded as a polymeric system. The stereoregularity (triad tacticity) was determined by use of NMR spectroscopy: ^{19}F-NMR spectra were recorded by use of a 282-MHz ^{19}F-NMR spectrometer (Bruker, AC-300P), using acetone as a solvent and monofluorotrichloromethane ($CFCl_3$) as an internal standard for PF-H1-Fn-Y with n = 1−3 and PF-H1-Fn-H with n = 4,6,8, while those for the other insoluble PF-H1-Fn-Y polymers were measured in a molten state above T_m by use of a 93.7-MHz ^{19}F-NMR spectrometer (JOEL, FX-100), using trifluoroacetic acid (TFA) as an internal standard. Three splitting peaks attributing to the α-F region of the spectra were observed around −160 to −170 ppm with $CFCl_3$ reference and 80 to 90 ppm with TFA. Triad tacticities were estimated from the intensity ratios of the three peaks according to the method of Majumder and Harwood.[9] Triad tacticities were also determined from the characteristic three splitting peaks of α-CH_3 in the ^{1}H-NMR spectra for PM-H1-Fn-Y and the peaks of C═O in the ^{13}C-NMR spectra for PA-H1-Fn-Y.[10,11] Here, ^{1}H-NMR and ^{13}C-NMR spectra were measured by use of a 300-MHz ^{1}H-NMR spectrometer (Bruker, AC-300P) and a 75-MHz ^{13}C-NMR spectrometer (Bruker, AC-300P), respectively.

Thermal analyses were performed at a heating rate of 10 K min^{-1}, using a differential scanning calorimeter (Perkin-Elmer, DSC-7). T_g was determined by the middle point of inflection in the heat capacity step on the first heating curve. T_m was determined as the temperature exhibiting the top of the endothermic peak.

X-ray diffraction patterns were taken by the following two methods: (1) X-ray diffraction patterns at room temperature were measured with an X-ray diffractometer (RU-3/RAD-rA, Rigaku Denki Co.), using monochromatic Cu Kα radiation (40 kV, 70/100 mA). The diffracted X-rays were detected by a photographic flat film at a distance of about 90 mm from the surface of the sheet samples by a normal-beam-transmission technique. The photograph was taken under vacuum to suppress the scattering of X-rays by air, where the exposure time was 1−2 h. To confirm the values of the Bragg spacings, the X-ray scatterings were also measured by a reflection method, where the scattering intensities were detected by a scintillation counter with a pulse-height analyzer. (2) For the X-ray measurements at elevated temperatures, the scattering intensities were detected by a scintillation counter using monochromatic Cu Kα radiation (50 kV, 280 mA) by a normal-beam-transmission technique. In addition, the patterns were also taken on a recording system with IPs (imaging plates) developed by Dr. Kawaguchi and his colleagues of Kyoto Uuniversity.[12] X-ray scattering measurements for the uniaxially drawn sheets were also performed along the equatorial and meridional directions, respectively, after adjusting the drawing direction to the meridional direction.

The polarizing infrared (IR) spectra were measured with a Perkin-Elmer 1640 FT-IR spectrophotometer, using a KRS-5 polarizer.

Results

Room-Temperature X-ray Diffractions. Figure 2 shows wide-angle X-ray diffraction intensity−Bragg angle (2θ) curves for (a) PF-H1-Fn-Y homologues and (b) several short fluoroalkyl PA-H1-Fn-Y and PM-H1-Fn-Y homologues. The short fluoroalkyl PA-H1-Fn-Y and PM-H1-Fn-Y homologues show only one diffuse scattering at a spacing between 0.43 and 0.53 nm, indicating that these polymers are noncrystalline, and this result is consistent with the previous results reported by several researchers,[1,2] in which the homologues did not form ordered structures or crystallites, when $N_c \leq 7$. On the other hand, PF-H1-Fn-Y homologues show a few scattering peaks in the low-angle region in addition to one or two intensive peaks in the high-angle region. Therefore, PF-H1-Fn-Y homologues are certainly crystalline even in the shorter fluoroalkyl side chains with $N_c \leq 5$, as reported in our previous communication.[7] As is easily seen in Figures 2a, the diffraction pattern depends on the length (N_c) and chemical structure of fluoroalkyl side chains, and moreover, the diffraction patterns for the shorter fluoroalkyl homologues (N_c<7) differ from those for the longer fluoroalkyl homologues. PF-H1-F2-H and PF-H1-F4-

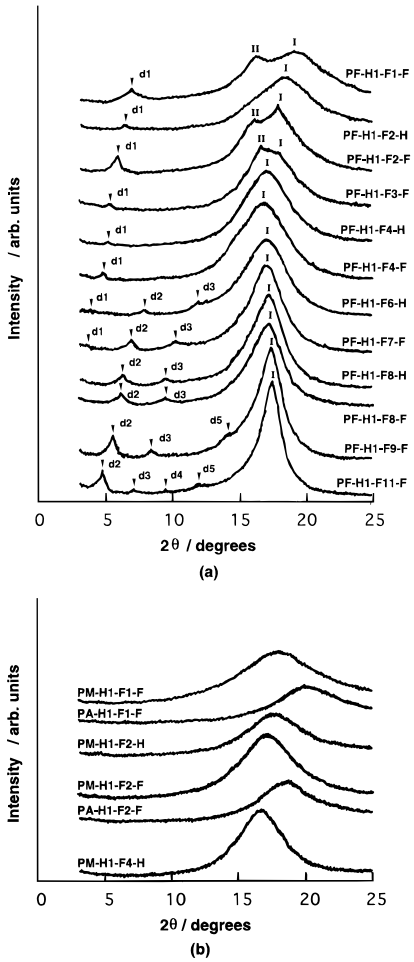

Figure 2. X-ray scattering intensity−Bragg angle (2θ) curves at room temperature: (a) PF-H1-Fn-Y homologues; (b) PM-H1-Fn-Y and PA-H1-Fn-Y homologues.

H, which have CF_2H in the end group of the side chains, have one low-angle scattering peak ($d1$) at 1.33 and 1.68 nm, respectively, and a high-angle scattering peak (I) at 0.48 and 0.52 nm, respectively, while PF-H1-F1-F, PF-H1-F2-F, and PF-H1-F3-F, whose end groups of the side chains are CF_3, have another high-angle peak denoted II at 0.54 nm, in addition to the peak I. In PF-H1-F1-F and PF-H1-F2-F, peak II is seen as a shoulder at the lower-angle side of the intense high-angle peak I, whereas in PF-H1-F3-F, it appears to be more intense than peak I. In PF-H1-F4-F with a CF_3 end group in the side chains, peak II was scarecely observed. On the other hand, more than three low-angle scattering peaks and one high-angle peak I are observed for the longer fluoroalkyl homologues with $N_c \geq 7$. Peak I becomes more intense and sharper with increasing N_c. We took X-ray diffraction photographs at room temperature for all the polymers to investigate the diffraction patterns in the low-angle region 3° below 2θ and ascertain some very weak peaks. Six typical photographs are illustrated in Figure 3, where the sketches of diffraction Debye rings are made in right part of the photographs. Photographs a and b of Figure 3 indicate that the shorter fluoroalkyl homologues ($N_c < 7$) have only one ring in the low-angle regions, corresponding to $d1$ in Figure 2, and the high-angle diffraction rings (I and II) faithfully correspond to those of Figure 2a; I and II rings are distinctly seen in part a for PF-H1-F4-F, whereas only I ring is seen in part b for PF-H1-F4-H. In parts d−f for the longer fluoroalkyl homologues, the photographs involve a few new data not seen in Figure 2a.

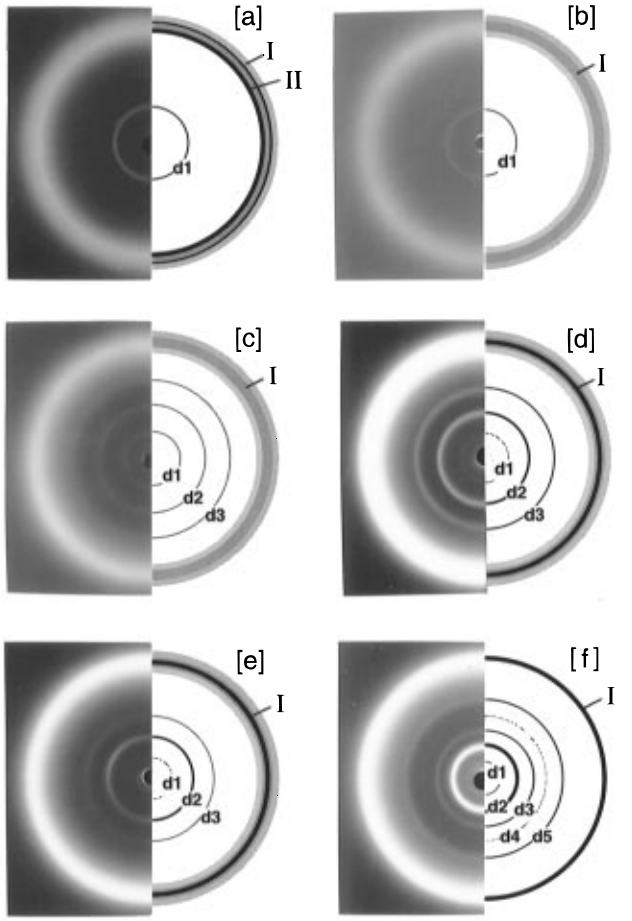

Figure 3. Room-temperature X-ray diffraction patterns of several poly(1*H*,1*H*-fluoroalkyl α-fluoroacrylate)s (PF-H1-Fn-Y): (a) PF-H1-F3-F; (b) PF-H1-F4-H; (c) PF-H1-F6-H; (d) PF-H1-F7-F; (e) PF-H1-F8-H; (f) PF-H1-F11-F. (The distance from the dry/plate to the surface of sample is about 90 mm but somewhat differs in the photographs.)

They show innermost rings ($d1$), but the $d1$ rings are extremely weak, compared with the intense $d2$ rings, and five rings, $d1-d5$, are observed in part f for PF-H1-F11-F. In PF-H1-F6-H (part c), $d1$, $d2$, and $d3$ are also observed, but they are weak.

Table 2 summarizes Bragg spacings and intensities of X-ray diffraction peaks in all PF-H1-Fn-Y homologues. From these diffraction data, PF-H1-Fn-Y homologues are roughly classified into two groups in terms of the length of the fluoroalkyl groups; the inner rings are mostly single when $N_c < 7$ and from triplet to quintet when $N_c \geq 7$. The ratio of three spacings for the first three inner diffractions for PF-H1-Fn-Y homologues with the long side chains ($N_c \geq 7$) is about $1:1/2:1/3$, showing the existence of a layered structure; the values of $d2$ and $d1$ fairly well coincided with the side chain length and twice that value, respectively, where the side chain length was calculated by the Coury−Pauling−Koltun molecular models. In Figure 4, three spacings, $d1$, $d2$, and $d3$, are plotted against N_c for two homologues, PF-H1-Fn-F and PF-H1-Fn-H, whose end groups of the fluoroalkyl side chains are CF_3 (circle) and CF_2H (triangle), respectively. The plots for both homologues show straight lines over a wide range of N_c, where the solid and broken lines were obtained by the least-squares fits. The increment of $d1$ and $d2$ per one CF_2 group of the side chains are estimated at about 0.22 and 0.14 nm for PF-H1-Fn-F with the end group of CF_3, respectively, and 0.26 and 0.15 nm for PF-H1-Fn-H with

Table 2. Bragg Spacings (nm) and Intensities of Poly(1*H*,1*H*-fluoroalkyl α-fluoroacrylate)s (PF-H1-Fn-Y) at Room Temperature

	diffraction maxima (/nm) and intensity[a]						
sample	d1	d2	d3	d4	d5	II[b]	I[b]
PF-H1-F1-F	1.26 ± 0.04 s					0.54m	0.45 m.d
PF-H1-F2-H	1.33 ± 0.07 vw, d						0.48 m, d
PF-H1-F2-F	1.48 ± 0.01 s					0.54 m	0.50 s
PF-H1-F3-F	1.66 ± 0.05 s					0.54 s	0.51 s, d
PF-H1-F4-H	1.68 ± 0.03 vw						0.52 s, d
PF-H1-F4-F	1.80 ± 0.07 m						0.52 s, d
PF-H1-F6-H	2.22 ± 0.09 vw, d	1.10 ± 0.03 vw, d	0.74 ± 0.01 vw, d				0.51 s, d
PF-H1-F7-F	2.5 ± 0.1 vw, d	1.28 ± 0.05 s	0.86 ± 0.03 m				0.52 vs, d
PF-H1-F8-H	2.9 ± 0.1 vw, d	1.40 ± 0.05 s	0.94 ± 0.02 m				0.52 vs, d
PF-H1-F8-F	2.8 ± 0.1 vw, d	1.41 ± 0.05 s	0.94 ± 0.02 m				0.52 vs
PF-H1-F9-F	2.9 ± 0.2 vw, d	1.57 ± 0.03 vs	1.04 ± 0.03 m		0.62 ± 0.02 vw		0.51 vs
PF-H1-F11-F	3.5 ± 0.2 vw, d	1.82 ± 0.03 vs	1.23 ± 0.03 m	0.95 ± 0.05 vw	0.74 ± 0.01 m		0.51 vs

[a] vs, very strong; s, strong; m, moderate; w, weak; vw, very weak; d, diffuse. [b] ±0.005.

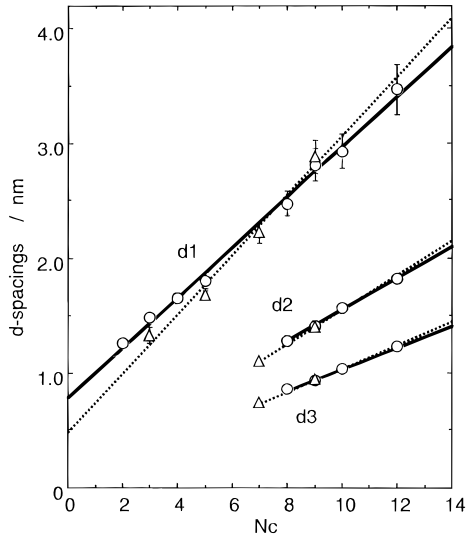

Figure 4. Dependences of the *d*-spacings (*d*1, *d*2, *d*3) on the carbon number (N_c) of the side groups of poly(1*H*,1*H*-fluoroalkyl α-fluoroacrylate)s (PF-H1-Fn-Y), Y = F (circle), Y = H (triangle), and the solid and broken lines were obtained by least-squares calculations. For PF-H1-Fn-F homologues, $d1 = 0.78 + 0.22N_c$ (correlation coefficient = 0.995) and $d2 = 0.19 + 0.14N_c$ (correlation coefficient = 0.998). For PF-H1-Fn-H homologues, $d1 = 0.47 + 0.26N_c$ (correlation coefficient = 0.983) and $d2 = 0.05 + 0.15N_c$.

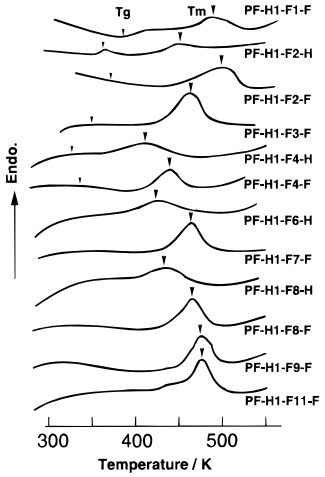

Figure 5. DSC heating curves of poly(1*H*,1*H*-fluoroalkyl α-fluoroacrylate)s (PF-H1-Fn-Y) at a rate of 10K min^{-1}.

the end group of CF_2H, respectively. The increment of *d*2 values is almost consistent with the length (0.13 nm) per CF_2 unit in polytetrafluoroethylene (PTFE), while the increment of *d*1 values is about twice as long as the length, although the increment of *d*1 for PF-H1-Fn-F homologues is a little smaller. Thus we conclude that PF-H1-Fn-F contains a double-layer packing of the fluoroalkyl side chains, which are almost perpendicular to the main chains. In the longer fluoroalkyl homologues, however, the single-layer packing structure may dominate, because the diffractive intensities of the rings *d1* are extremely weak, compared with those of the rings *d*2.

As already mentioned in the Introduction, in the fluoroalkyl acrylate and methacrylate polymers, the ordered structures composed of layer packings of the side chains have been found only for the longer fluoroalkyl homologues ($N_c = 1 + n \geq 8$) and not for the shorter fluoroalkyl homologues. It is, therefore, noteworthy that even in the short fluoroalkyl side chains with $N_c \leq 5$, poly(1*H*,1*H*-fluoroalkyl α-fluoroacrylate)s form the double-layered structure.

DSC Data. Figure 5 shows DSC heating curves for PF-H1-Fn-Y. All the homologues exhibit an endothermic peak corresponding to the melting of crystallites. These endothermic peaks are broad and are accompanied with a rather small enthalpy change but were well-reproducible. The shorter fluoroalkyl PA-H1-Fn-Y and PM-H1-Fn-Y homologues ($N_c \leq 5$) did not show any endothermic transitions. Therefore, the DSC data confirm the X-ray diffraction results that the short fluoroalkyl PA-H1-Fn-Y and PM-H1-Fn-Y homologues are noncrystalline but all the homologues are crystalline in the PF-H1-Fn-F system. The melting points (T_m) of crystallites and their enthalpy changes (ΔH_m) are estimated from the DSC peaks. In the shorter fluoroalkyl PF-H1-Fn-Y homologues, the DSC curves show other small changes below T_m, which are attributable to the glass transitions of amorphous regions.

The variations of T_m, ΔH_m (in kJ mol^{-1}, based on monomer unit), and T_g with N_c are shown in Figure 6. The values of T_m and ΔH_m are significantly dependent upon both length of fluoroalkyl side chain (N_c) and substituent Y in the end group of the side chains. In the shorter fluoroalkyl side chain region ($N_c \leq 5$), T_m rapidly decreases with increasing N_c but gradually increases when N_c increases beyond 5, showing a minimal value near $N_c = 5$. This variation of T_m with N_c is seen for both PF-H1-Fn-F and PF-H1-Fn-H homologues. However, the values of T_m for PF-H1-Fn-H homologues (Y = H) are lower than those for PF-H1-Fn-F homologues (Y = F). On the other hand, a variation of ΔH_m with N_c differs with the substituent Y. In PF-H1-Fn-F homologues, ΔH_m shows a minimal value near $N_c = 5$ and increases with increasing N_c

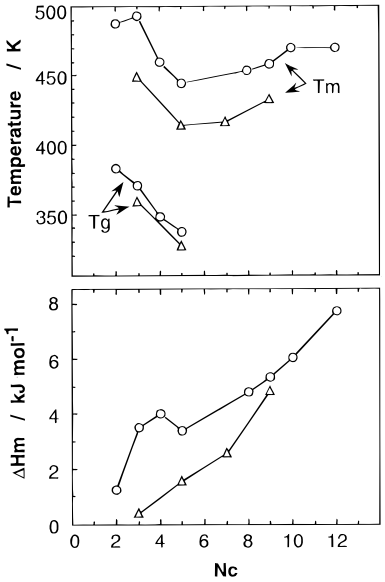

Figure 6. Dependences of melting peak temperatures (T_m), glass transition temperatures (T_g), and enthalpy changes of melting (ΔH_m in kJ mol^{-1}) of poly(1*H*,1*H*-fluoroalkyl α-fluoroacrylate)s (PF-H1-Fn-Y) on the carbon number (N_c) of the side chains: Y = F (circle), H (triangle).

above 5, while in PF-H1-Fn-H homologues, ΔH_m increases monotonously with increasing N_c. The values of ΔH_m for PF-H1-Fn-H are considerably smaller, compared with those for PF-H1-Fn-F. These results suggest that the crystallinity for PF-H1-Fn-H homologues is lower than that for PF-H1-Fn-F homologues, which wsa also confirmed by the X-ray diffraction results in the previous section. We also performed DSC measurements for the samples annealed enough at a temperature between T_g and T_m. In each sample, T_m was almost unchanged but ΔH_m increased with annealing. However, the relationships of ΔH_m with N_c described above were held for these annealed samples. Consequently, the presence of a minimal value of T_m near $N_c = 5$ suggests that the structure of crystallites for the shorter fluoroalkyl homologues is different from that for the longer fluoroalkyl homologues ($N_c \geq 7$), which again corresponds to the previous X-ray diffraction results. T_g monotonously decreases with increasing N_c but was not determined for the longer side chain region, because of unclear DSC curves.

Polarized IR Spectra for Uniaxially Drawn Samples. Figure 7 illustrates polarized IR spectra in the carbonyl stretching region of uniaxially drawn PF-H1-Fn-F and PM-H1-Fn-F films. PM-H1-F2-F shows one absorption peak near 1749 cm^{-1} and PF-H1-F2-F shows two splitting peaks near 1772 and 1798 cm^{-1}. The peaks for PF-H1-F2-F shift by about 23−49 cm^{-1} to higher wavenumbers than that for PM-H1-F2-F, which would be due to the electron-withdrawing effect of the fluorine atom in the α-position of the acrylate moiety. The splitting of the C═O stretching peak has been also observed for poly(alkyl α-chloroacrylate)s by several researchers.[13,14] On the other hand, the drawn PM-H1-F2-F film shows no dichroism for the C═O stretching band but the drawn PF-H1-F2-F have a distinct dichroism; in PF-H1-F2-F, the two splitting absorption peaks at 1772 and 1798 cm^{-1} are more intense in the perpendicular direction to the drawing direction than in the parallel direction. Moreover, as seen in Figure 7, the larger the drawing ratio is, the smaller the dichroic ratio becomes, where the dichroic ratio is estimated as $A_{||}/A_{\perp}$($A_{||}$ and $A_{\perp}$ are absorbances in the parallel and perpendicular directions, respectively). Although the C═O bands originate from both the amorphous and crystalline regions, the presence of the perpendicular dichroism in the C═O bands indicates that the C═O bonds in the crystallites arrange preferentially perpendicular to the main chains, being consistent with the anisotropic X-ray diffraction results as is mentioned in the subsequent section. These infrared dichroism results suggest that PF-H1-Fn-Y homologues with the shorter side chains have an ordered structure in which the main backbone chains including the C═O moieties arrange each other to some extent.

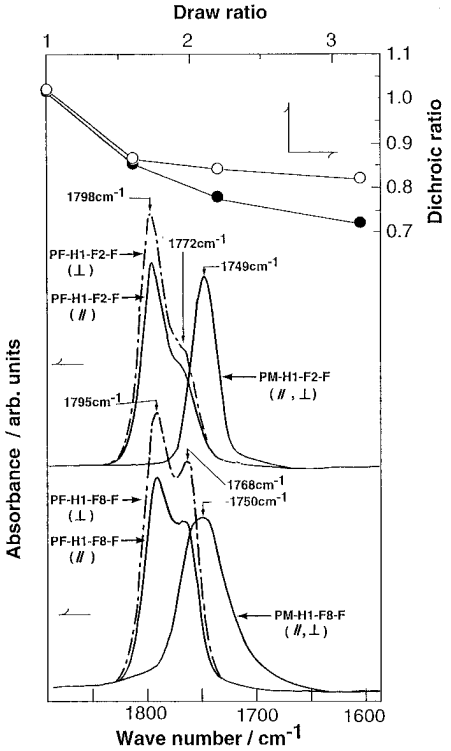

Figure 7. Carbonyl absorptions in polarized IR spectra for uniaxially drawn samples of PF-H1-Fn-F (n = 2 and 8) and the corresponding PM-H1-FnhF (n = 2 and 8), the electric vector is parallel (||) and perpendicular (⊥) to the drawing direction, and plots of dichroic ratios in the absorbances at 1772 (circle) and 1798 (black circle) cm^{-1} versus draw ratios for PF-H1-F2-F.

The perpendicular dichroism for PF-H1-F8-F and PM-H1-F8-F is similar to that for the short fluoroalkyl homologues (PF-H1-F2-F and PM-H1-F2-F); in PF-H1-F8-F, the absorption intensity is larger in the perpendicular direction ($A_{\perp}$) to the drawn direction than in the parallel direction ($A_{||}$), but shows no dichroism in PM-H1-F8-F. This spectral result suggests that the main backbone chains of PF-H1-Fn-Y are ordered even in the longer fluoroalkyl homologues.

X-ray Diffraction for Uniaxially Drawn Samples and Temperature Dependence of X-ray Diffraction. As is already described, PF-H1-Fn-Y homologues show crystalline properties even in the short fluoroalkyl homologues ($N_c \leq 5$) at room temperature, while the short PA-H1-Fn-Y and PM-H1-Fn-Y homologues are noncrystalline. Figure 8a illustrates X-ray scattering intensity−Bragg angle curves at room temperature for uniaxially drawn PF-H1-Fn-Y homologues. Parts b and c of Figure 8 show X-ray diffraction photographs for two uniaxially drawn homologues, (b) PF-H1-F1-F and (c) PF-H1-F8-F, respectively, which are typical examples

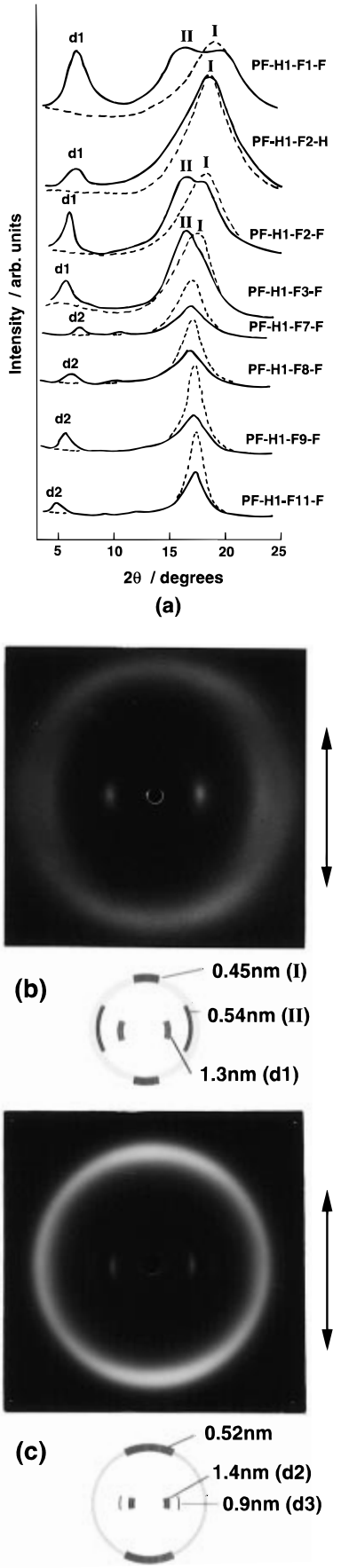

Figure 8. Room-temperature X-ray scattering curves of uniaxially drawn samples of (a) PF-H1-Fn-Y, the solid and broken curves indicate perpendicular and parallel directions to the drawing direction, respectively, and the diffraction patterns of (b) PF-H1-F1-F and (c) PF-H1-F8-F, the arrow indicates the drawing direction.

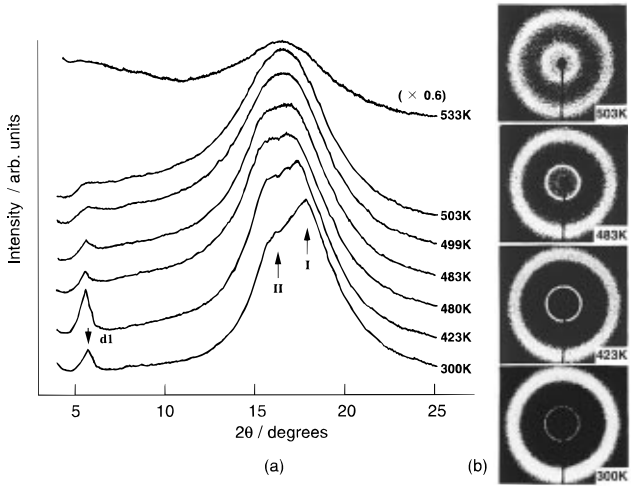

Figure 9. (a) X-ray scattering curves at different temperatures for PF-H1-F2-F, and (b) several diffraction patterns recorded on IPs (imaging plates).

of the short and long fluoroalkyl homologues, respectively. In parts b and c of Figure 8, the inner rings at 1.3 nm and at 1.4 and 0.9 nm, respectively, are strengthened perpendicular to the drawing (meridional) direction, i.e., parallel to the equatorial direction, which indicates that the fluoroalkyl side chains arrange almost perpendicular to the main chains. In the outer rings I (0.45 and 0.52 nm, respectively), their intensities are more intense in the meridional direction than in the equatorial direction, indicating that the outer rings I may come from a later ordering between the fluoroalkyl side chains in the layers. These results support that the main backbone chains arrange in the parallel direction to the drawing direction, and the fluoroalkyl chains are packed perpendicular to the main chain to form crystallites. As pointed out already, the short fluoroalkyl PF-H1-Fn-F homologues with Y = F tend to exhibit the scattering peak II in addition to peak I in the high-angle region. Figure 8a,b also reveals that the scattering peaks (outer ring) II give a characteristic anisotropy for the drawn PF-H1-F1-F, PF-H1-F2-F, and PF-H1-F3-F. The intensity of each peak (ring) II is more intense in the equatorial direction than in the meridional direction, contrary to that of peak (ring) I. The anisotropy of the peak (ring) II suggests that the main backbone chains arrange each other to form an ordered structure in those polymers.

Figure 9 shows (a) X-ray scattering curves and (b) some diffraction patterns recorded on IPs for PF-H1-F2-F at elevated temperatures. At 300 K, the scattering curves showed one low-angle peak (inner ring) *d1* near $2\theta = 5°$ and two high-angle peaks (outer rings) I and II between 15 and 20°. As the temperature is raised to 423 K, both the low-angle peak (*d1*) and two high-angle peaks (I, II) somewhat shift to the lower-angle side, and the intensity of peak *d*1 obviously becomes more intense, which is also observed in the pattern of IP. As the temperature increases more from 423 K, the intensity of peak *d*1 is weakened and somewhat broader, and the peaks I and II prefer to join. At 499 K above T_m (493K), peaks I and II become one diffuse peak, whereas, interestingly, peak *d1* becomes diffuse and weak but still remains. The trace of the peak *d1* is observed even at 503 K, which is also confirmed on the IP pattern, but disappears at 533 K. In Figure 10, the spacing of these three peaks is plotted against temperature. This clearly shows that peaks I and II, which are attributable to the later order in the fluoroalkyl side groups and the

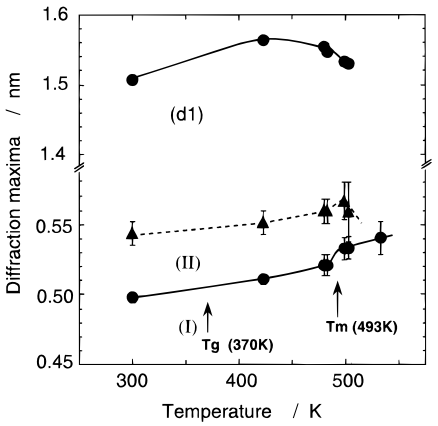

Figure 10. Temperature dependences of the *d*-spacings of one low-angle (*d*1) and two high-angle (I, II) diffraction maxima observed in the X-ray scattering curves of PF-H1-F2-F.

ordering of main backbone chains, respectively, tend to unite into one diffuse peak in the melting state above T_m.

In Figure 9, it is noted that the intensity of the peak *d1*, corresponding to the double layered structure of the fluoroalkyl side chains, is strengthened with increasing temperature from 300 to 423 K and above 423 K weakened, and, as a result, the intensity shows a maximal value around 423 K above T_g (370 K). As already described, the short fluoroalkyl PF-H1-Fn-Y homologues have crystallites below T_m in which both fluoroalkyl side chains and main backbone chains are arranged. However, at room temperature, the arrangements of main chains may restrict the ordering of the side chains. With increasing temperature, the arrangements of main chains may be relaxed, which makes it possible for the side chains to be more closely packed, leading to the increase in the intensity of peak *d*1. The relaxation in the packings of main chains with temperature would be accelerated above T_g (370 K for PF-H1-F2-F), and this relaxation may result in promoting the ordering of the side chains, i.e., producing the maximal intensity of peak *d*1 around 423 K. The presence of the diffuse *d*1 peak above T_m suggests that some ordering corresponding to a double-layer packing still remains. Since this ordering is considerably disturbed, we think that the ordering state above T_m is a mesomorphic state reminiscent of a smectic A phase.

It is an interesting question why the shorter fluoroalkyl PF-H1-Fn-Y homologues exhibit crystalline properties, while the shorter fluoroalkyl PA-H1-Fn-Y and PM-H1-Fn-Y homologues are noncrystalline. The present study reveals that the crystallites of the shorter fluoroalkyl PF-H1-Fn-Y homologues are constructed by both fluoroalkyl side chains and main backbone chains. We think that the αC−F bond in the main backbone chains may enhance an intermolecular interaction, and this interaction would produce an ordered packing of the main chains, because the chemical structure of PF-H1-Fn-Y differs only in the existence of the polar αC−F bond from those of PA-H1-Fn-Y and PM-H1-Fn-Y. In other words, the crystallizable main chains impose a double-layer packing of the short fluoroalkyl side chains.

On the other hand, it is well-known that crystallinity in acrylate polymers depends on the stereoregularity. The triad tacticity somewhat differs by the type of polymers as seen in Table 1 (the isotacticity (mm) increases in the order PF-H1-Fn-Y (n = 1−4) > PM-H1-Fn-Y (n = 1−4) > PA-H1-Fn-Y (n = 1,2), and the syndiotacticity (rr) is in the order PM-H1-Fn-Y > PF-H1-Fn-Y > PA-H1-Fn-Y), but it is considered to be substantially atactic for all the polymers used here. The small differences in tacticity seem not to be correlated with the differences in crystallinity among these three types of polymers. Therefore, the stereoregularity appears not to be directly related to whether the polymers are crystalline or not. Noticeably, the crystallinity of PF-H1-Fn-Y homologues with $N_c \leq 5$ depends on both the length of the fluoroalkyl side chains and the type of their end groups (Y); the crystallinity of PF-H1-F2-H, whose end group of the side chains is CF_2H, is much lower than that of PF-H1-F1-F and PF-H1-F2-F. According to our previous dielectric work for PF-H1-Fn-Y,[6] α-relaxation, which is assigned to a reorientational motion of long segments containing the backbone chains in the amorphous region, was observed at high temperatures above T_g at 10 kHz and was 30−50 K lower in the PF-H1-Fn-H homologues than in the PF-H1-Fn-F homologues. The α-relaxation may be depressed by the crystalline region and so appeared at much higher temperatures above T_g in the audio frequencies. Therefore the CF_2H end group is considered to disturb the ordering of the main chains, causing the lowering in crystallinity and relaxation temperatures by the polar nature of this end group. Moreover, we found that the relaxation temperatures decreased with increasing length of fluoroalkyl side chains, for example, from 443 K for PF-H1-F1-F (N_c = 2) to 435 K for PF-H1-F2-F (N_c = 3). T_g determined by DSC also decreased from 383K for PF-H1-F1-F (N_c = 2) to 336K for PF-H1-F4-F (N_c = 5). These decreases in relaxation temperatures and T_g may be explained by a plasticizing effect of the fluoroalkyl side chains.

In the long fluoroalkyl PF-H1-Fn-Y homologues with $N_c \geq 7$, the fluoroalkyl side chains are packed with each other to form mostly a single-layered structure at room temperature, while the side chains form a double-layered structure in the shorter fluoroalkyl homologues; when $N_c \leq 5$, the strong *d*1 ring is seen, whereas when $N_c \geq 8$, ring *d*1 is extremely depressed and ring *d*2 becomes predominant, as shown in Figure 3. At N_c = 7, the intensity of ring *d*1 is comparable to that of ring *d*2, which may indicate that single- and double-layer packings coexist in the N_c = 7 homologue (PF-H1-F6-H). The layered structure changes around N_c = 7 from a double-layer packing for the shorter fluoroalkyl homologues to a single-layer packing for the longer fluoroalkyl homologues, when N_c increases. Okawara et al.[3] reported that poly(fluoroalkyl acrylate)s with the side chains of $(CH_2)_2(CF_2)_nF$ (PA-H2-Fn-F, $N_c = 2 + n = 10-14$) form a considerably perfect double-layered structure, where the fluoroalkyl side chains are packed in a hexagonal lattice. In PA-H2-F8-F, the lateral distance of the side chains in layers was 0.50 nm,[5,8] very close to 0.49 nm in PTFE,[15] but ranges between 0.51 and 0.52 nm in the present PF-H1-Fn-Y (n = 7−10) (see Table 2). The value of ΔH_m was about 8.1 kJ mol^{-1} for PA-H2-F8-F but 5.3−6.0 kJ mol^{-1} for PF-H1-Fn-Y (n = 8,9). That is, the long fluoroalkyl PF-H1-Fn-Y homologues have a bit of larger lateral distances and smaller ΔH_m values, compared with those of PA-H2-F8-F. These results suggest that the layered structure of PF-H1-Fn-Y homologues (n = 8,9) is a little more disturbed than that of PA-H2-F8-F. The polarized IR spectra of uniaxially drawn films (Figure 7) showed a perpendicular dichroism for the long fluoroalkyl PF-H1-F8-F homologue, and the longer fluoroalkyl PF-H1-Fn-Y homologues, therefore, were concluded to have crystallites

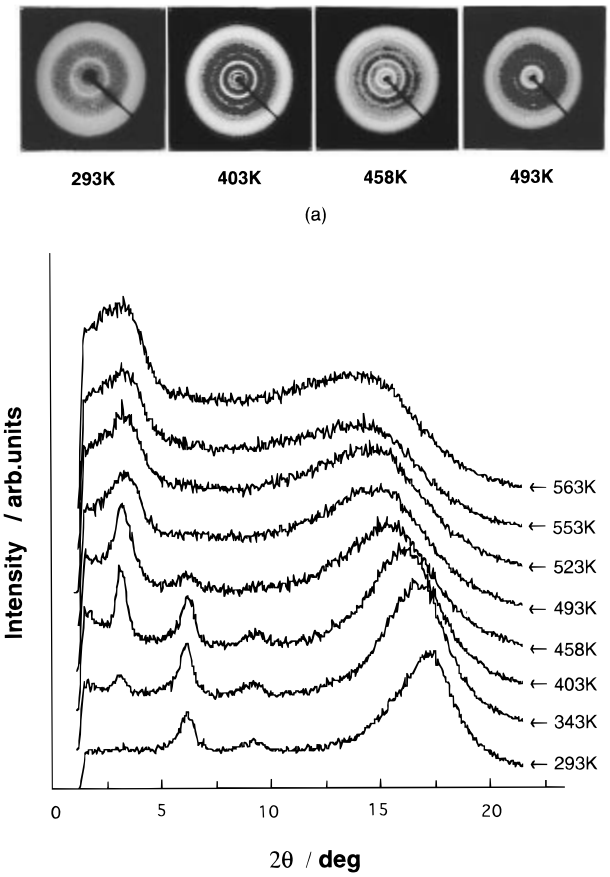

Figure 11. (a) Several X-ray diffraction patterns recorded on IPs (imaging plates) at elevated temperatures for PF-H1-F8-F, and (b) the scattering curves digitally converted from all the IP patterns measured.

consisting of not only fluoroalkyl side chains but also main backbone chains.

Figure 11 illustrates (a) X-ray diffraction patterns recorded on IPs for PF-H1-F8-F at elevated temperatures and (b) the scattering curves digitally converted from all the IP patterns measured. At room temperature, the polymer has a single-layer packing (see the peak at $2\theta = \sim 6°$), but when temperature is raised, the packing transforms into a double-layer packing (see the peak at $2\theta = \sim 3°$) in the temperature range probably near and above T_g. (T_g is estimated below 403K by a dynamic mechanical measurement.[16]) The ordering of the double-layer packing distinctly remains at and above T_m. These results indicate that the ordering of the main backbone chains perturbs the layered ordering of the fluoroalkyl side chains to form a single-layer packing at room temperature. When the temperature is increased from room temperature, however, the ordering of the rigid main backbone chains would be relaxed above T_g, and then the packing of fluoroalkyl side chains may be rearranged to transform into a double-layer packing. The existence of double-layer packing above T_m suggests that the polymers are in a mesomorphic state above T_m, as also seen in Figure 9 for PF-H1-F2-F.

Discussion

Ordered structure was studied for a homologous series of poly(1*H*,1*H*-fluoroalkyl α-fluoroacrylate)s [PF-H1-Fn-Y, Y = H or F, $N_c = 1 + n = 2-12$] by use of X-ray diffractions, DSC, and polarized IR spectral techniques. The present results clearly indicate the presence of crystallites for all the homologues, and noticeably the crystallites exist even in the short fluoroalkyl homologues with $N_c \leq 5$.

In this work, we found that the structure of the crystallites is distinctly divided into the following two classes by the length of the fluoroalkyl side chains: (1) At room temperature, in the short fluoroalkyl homologues whose N_c is probably less than 7, the fluoroalkyl side chains are arranged into a double-layer packing. As the temperature increases, the double-layer packing is more ordered around a temperature above T_g and then gradually disordered. However, the double-layer packing is largely disturbed in some higher temperature range above T_m but still faintly remains and completely disappears at higher temperatures, which suggests the existence of a mesophase reminiscent of a smectic A phase above T_m. (2) In the long fluoroalkyl homologues whose N_c is larger than 7, the fluoroalkyl side chains are packed mostly into a single-layered structure at room temperature, but the single-layer packing transformed into a double-layer packing with increasing temperature above T_g. In the $N_c = 7$ homologue, the packing of the side chains forms an intermediate layered structure.

In this work, it is to be emphasized that the main backbone chains are packed into the crystallites to form an ordered structure for all the PF-H1-Fn-F homologues. In the short fluoroalkyl homologues, the ordering of the main backbone chains is considered to govern the structure of the crystallites. With increasing temperature, the rigid main backbone chains are softened and relaxed above T_g and then the double-layer packing by the fluoroalkyl side chains may be more ordered. When temperature is increased more, the ordering of the fluoroalkyl side chains may be gradually disturbed. On the other hand, the higher degree of ordering of the fluoroalkyl side chains may prevail in the longer fluoroalkyl homologues ($N_c \geq 8$) at room temperature, but the ordering of main backbone chains may somewhat disturb the packing of the fluoroalkyl side chains, resulting in a single-layered structure. With increasing temperature, the ordering of the fluoroalkyl side chains may become predominant due to the relaxation or softening of the ordering of the main backbone chains above T_g, and this mauy cause the transformation from single-layer packing to double-layer packing. Furthermore, the short fluoroalkyl PA-H1-Fn-Y and PM-H1-Fn-Y ($N_c < 8$), having H and CH_3 at the α-position of the acrylate moiety, respectively, are noncrystalline, while the long fluoroalkyl homologues ($N_c \geq 8$) are crystalline and have the layered structure formed by the long side chains. However, it is to noted that PA-H1-Fn-Y and PM-H1-Fn-Y homologues do not exhibit any ordering of the main backbone chains.

In the previous work,[8] we investigated the layered structure and its change with temperature of poly(1*H*,1*H*,2*H*,2*H*-perfluorodecyl α-substituted acrylate)s [$-\{CH_2CXC(O)O(CH_2)_2(CF_2)_8F\}_p-$, X = F, Cl, CH_3, H] (PX-H2-F8-F, X = F, C, M, A). At room temperature, the layered structure was in a double-layer packing in PA-H2-F8-F, in both single- and double-layer packings in PM-H2-F8-F, and in a single-layer packing in PF-H2-F8-F and PC-H2-F8-F, respectively. As temperature increases, in PF-H2-F8-F and PC-H2-F8-F, the single-layer packing transformed into a double-layer packing around a temperature between T_g and T_m, and in PF-H2-F8-F, the double-layer packing remained even in the higher temperature range (about 80 K) above T_m. These

structural changes with temperature are very similar to those for PF-H1-F8-F found in this work. On the other hand, both double- and single-layer packings in PM-H2-F8-F and the double-layer packing in PA-H2-F8-F completely disappeared around T_m, which indicates the meltings of the crystallites formed only by the side chains. Thus, we can conclude that the ordering of the main backbone chains occurs in two PF-Hm-Fn-Y homologues whose alkylene groups of the side chains are methylene ($m = 1$) or ethylene ($m = 2$). However, it should be noted that there is a significant difference in enthalpy change between PF-H1-F8-F and PF-H2-F8-F (5.3 and 2.3 kJ mol^{-1}, respectively). The difference may be caused by the degree of ordering of the main backbone chains. The effect of alkylene groups on the ordering of main chains will be discussed elsewhere.

Acknowledgment. We very much thank Dr. S. Koizumi (Mitsuboshi Co. Ltd., Osaka, Japan), Professor Dr. K. Tadano (Gifu College of Medical Technology, Gifu, Japan), and Professor Dr. M. Iwami (Okaywam University, Okayama, Japan) for helpful discussions and Professor Dr. A. Kawaguchi (Ritsumeikan University, Shiga, Japan) and Dr. S. Murakami (The Institute for Chemical Research, Kyoto University, Kyoto, Japan) for invaluable suggestions in the X-ray studies. S.K. acknowledges the support of the Ministry of Education, Science, and Culture in Japan (Grant-in-Aid for Scientific Research No. 0570800).

References and Notes

(1) Ishiwari, K.; Ohmori, A.; Koizumi, S. *Nippon Kagaku Kaishi* **1985**, *10*, 1924.
(2) Budovskaya, L. D.; Ivanova, V. N.; Oskar, L. N.; Lukasov, S. V.; Baklagina, Yu. G.; Sidorovich, A. V.; Nasledov, D. M. *Vysokomol. Soedin., Ser. A* **1990**, *32*, 561.
(3) Oakwara, A.; Maekawa, T.; Ishida, Y.; Matsuo, M. *Polym. Prepr. Jpn.* **1991**, *40*, 3898.
(4) Boutevin, B.; Rousseau, A.; Bosc, D. *J. Polym. Sci. Part A, Polym. Chem.* **1992**, *30*, 1279.
(5) Volkov, V. V.; Platé, N. A.; Takahara, A.; Kajiyama, T.; Amaya, N.; Murata, Y. *Polymer* **1992**, *33*, 1316.
(6) Koizumi, S.; Tadano, K.; Tanaka, Y.; Shimizu, T.; Kutsumizu, S.; Yano, S. *Macromolecules* **1992**, *25*, 6563.
(7) Shimizu, T.; Tanaka, Y.; Kutsumizu, S.; Yano, S. *Macromolecules* **1993**, *26*, 6694.
(8) Shimizu, T.; Tanaka, Y.; Kutsumizu, S.; Yano, S. *Macromol. Symp.* **1994**, *82*, 173.
(9) Majumder, R. N.; Harwood, H. J. *Polym. Bull.* **1981**, *4*, 391.
(10) Bovey, F. A.; Tiers, G. V. D. *J. Polym. Sci.* **1960**, *44*, 173.
(11) Hatada, K. *Kobunshi* **1981**, *30*, 696.
(12) Kawaguchi, A.; Murakami, S.; Katayama, K.; Mihoichi, M.; Ohta, T. *Bull. Inst. Chem. Res., Kyoto Univ.* **1991**, *69*, 145.
(13) Wesslen, B.; Lenz, R. W. *Macromolecules* **1971**, *4*, 20.
(14) Dever, G. R.; Karasz, F. E.; Macknight, W. J.; Lenz, R. W. *J. Polym. Sci., Polym. Chem. Ed.* **1975**, *13*, 2151.
(15) Chazy, H.; Smith, P. *J. Polym. Sci., Polym. Lett. Ed.* **1986**, *24*, 557.
(16) Shimizu, T.; et al., unpublished data.

MA950746V